



## Challenges and limitations of the $^{210}\text{Pb}$ sediment dating method: Results from an IAEA modelling interlaboratory comparison exercise

M. Barsanti<sup>a,\*</sup>, R. Garcia-Tenorio<sup>b</sup>, A. Schirone<sup>a</sup>, M. Rozmaric<sup>c</sup>, A.C. Ruiz-Fernández<sup>d</sup>, J. A. Sanchez-Cabeza<sup>d</sup>, I. Delbono<sup>a</sup>, F. Conte<sup>a</sup>, J.M. De Oliveira Godoy<sup>e</sup>, H. Heijnis<sup>f</sup>, M. Eriksson<sup>g</sup>, V. Hatje<sup>h</sup>, A. Laissaoui<sup>i</sup>, H.Q. Nguyen<sup>j</sup>, E. Okuku<sup>k</sup>, Saber A. Al-Rousan<sup>l</sup>, S. Uddin<sup>m</sup>, M.W. Yii<sup>n</sup>, I. Osvath<sup>c</sup>

<sup>a</sup> Italian National Agency for New Technologies, Energy and Sustainable Economic Development (ENEA), Italy

<sup>b</sup> Universidad de Sevilla, Centro Nacional de Aceleradores, Spain

<sup>c</sup> International Atomic Energy Agency (IAEA), Environment Laboratories, Monaco

<sup>d</sup> Unidad Académica Mazatlán, Instituto de Ciencias del Mar y Limnología, Universidad Nacional Autónoma de México, Mexico

<sup>e</sup> Pontificia Universidade Católica do Rio de Janeiro, Brazil

<sup>f</sup> Australian Nuclear Science and Technology Organization (ANSTO), Australia

<sup>g</sup> Linköping University, Sweden

<sup>h</sup> Centro Interdisciplinar de Energia e Ambiente (CIENAM), Universidade Federal da Bahia, Brazil

<sup>i</sup> Centre national de l'énergie, des sciences et des techniques nucléaires (CNESTEN), Morocco

<sup>j</sup> Viet Nam Atomic Energy Institute (VINATOM), Viet Nam

<sup>k</sup> Kenya Marine and Fisheries Research Institute (KMFRI), Kenya

<sup>l</sup> The University of Jordan, Department of Geology, Faculty of Science, Amman, Jordan

<sup>m</sup> Kuwait Institute for Scientific Research (KISR), Kuwait

<sup>n</sup> Malaysian Nuclear Agency, Malaysia

### ARTICLE INFO

#### Keywords:

Sediment cores

$^{210}\text{Pb}$  dating

$^{137}\text{Cs}$

Models

Validation

### ABSTRACT

The  $^{210}\text{Pb}$  sediment dating is the most widely used method to determine recent (~100–150 years) chronologies and sediment accumulation rates in aquatic environments and has been used effectively for reconstruction of diverse environmental processes associated with global change. Owing to the relative accessibility of the  $^{210}\text{Pb}$  methodology, many environmental chronologies have been produced, but not always critically assessed. Sometimes, sedimentary processes such as compaction, local mixing, erosion, or episodic sedimentation are not taken into account, nor the validity of the fundamental premises and proper estimation of uncertainties assessed. A Pb-210 dating interlaboratory comparison modelling exercise was designed within the framework of the IAEA (International Atomic Energy Agency) Coordinated Research Project “Study of temporal trends of pollution in selected coastal areas by the application of isotopic and nuclear tools” (CRP K41016), to identify potential problems associated with the use of  $^{210}\text{Pb}$  dating models and to suggest best practices to obtain reliable reconstructions. The exercise involved 14 laboratories worldwide with different levels of expertise in the application of the  $^{210}\text{Pb}$  dating methods. The dating exercise was performed using  $^{210}\text{Pb}$ ,  $^{226}\text{Ra}$  and  $^{137}\text{Cs}$  activity data from two sediment cores (coastal and lacustrine sediments), and the participants were requested to provide their  $^{210}\text{Pb}$  chronologies based on dating models. This modelling exercise evidenced the limitations and constraints of  $^{210}\text{Pb}$  method when supplementary and validation information is not available. The exercise highlighted the relevance of solid understanding of the fundamentals, assumptions and limitations of the  $^{210}\text{Pb}$  dating method and its validation, and allowed identifying key aspects to improve the reliability of  $^{210}\text{Pb}$  dating process, including: a critical examination and interpretation of the  $^{210}\text{Pb}$  activity depth profile; an appropriate selection of the  $^{210}\text{Pb}$  dating model according to the characteristics of the  $^{210}\text{Pb}$  activity profile and the environmental setting taking into account sediment compaction in the calculations; a sound identification of the  $^{210}\text{Pb}$  equilibrium depth and the estimation of the  $^{210}\text{Pb}$  inventory ensuring the best possible estimation of interpolated  $^{210}\text{Pb}$  values when needed; and the use of independent markers to corroborate the age models.

\* Corresponding author.

E-mail address: [mattia.barsanti@enea.it](mailto:mattia.barsanti@enea.it) (M. Barsanti).

<https://doi.org/10.1016/j.quageo.2020.101093>

Received 27 August 2019; Received in revised form 11 April 2020; Accepted 14 May 2020

Available online 29 May 2020

1871-1014/© 2020 Published by Elsevier B.V.

## 1. Introduction

Many coastal areas in proximity to urban, agricultural and industrial centres have been receiving increased loads of contaminants, such as trace elements, nutrients and organic compounds, as a result of rapid urbanization and increased population density. Contaminants are transported to coastal areas through submarine groundwater discharge, atmospheric and fluvial inputs from land-based activities. The continuous and increasing exploitation of coastal areas worldwide alters ecosystem structure and functioning and compromises human health. There is an urgent need for science-based policies to mitigate these problems, as advocated in the UN Sustainable Development Goals 14. To this effect, the knowledge on contamination sources, fate, levels and trends is essential for defining effective environmental protection measures.

Marine sediments effectively retain and preserve many of the aforementioned contaminants (e.g. GESAMP, 1994, 1987; Miralles et al., 2004; Martín et al., 2009; Alonso-Hernandez et al., 2015; Páez-Osuna et al., 2017). The use of these natural environmental archives, when properly dated (mostly by radiometric methods), allows the reconstruction of temporal trends of concentration levels, identification of relevant sources, controlling processes, and assessment of the contamination status of marine ecosystems. Radiometric analyses of marine sediments help to i) complement conventional monitoring programmes, and/or ii) reconstruct historical contamination levels, even when long-term monitoring data are missing (Sanchez-Cabeza and Druffel, 2009). Research on radiotracers in marine sediments has greatly contributed to the understanding of the contaminant profiles in the recent past, as well as environmental changes.

The  $^{210}\text{Pb}$  natural radionuclide is present in all environmental compartments and it has been applied as an environmental radiotracer of many processes: ocean biogeochemistry, atmospheric deposition and contamination (Sanchez-Cabeza and Ruiz-Fernández, 2012 and reference therein), sedimentary processes (Palinkas and Nittrouer, 2007; Delbono et al., 2016), to evaluate the recent impacts of microplastics (Turner et al., 2019) and the accumulation rates of sediment organic carbon, also termed blue carbon, for carbon dioxide sequestration in the environment (for example Arias-Ortiz et al., 2018).

Moreover, it has been more than 50 years since  $^{210}\text{Pb}$  was first introduced as a dating tool (Goldberg, 1963) and more than 45 years since the method was first applied to lacustrine (Krishnaswamy et al., 1971) and marine (Koide et al., 1972) sediments. Since then, the measurement of  $^{210}\text{Pb}$  in sediment cores has become a common method for determining sedimentation rates in various aquatic environments over a time-span of approximately 100–150 years. Various authors have further developed the  $^{210}\text{Pb}$  dating method and its application as a geochronological tool in sediment profiles by using conceptual models that are based on specific assumptions. The most common  $^{210}\text{Pb}$  dating models are the Constant Activity (CA, also known as Constant Initial Concentration, CIC), the Constant Flux and Constant Sedimentation rate (CFCs) and the Constant Flux (CF, also called Constant Rate of Supply, CRS) models (Appleby et al., 1979; Appleby and Oldfield, 1992, 1978; Robbins and Edgington, 1975). A comprehensive review of these dating models is presented in Sanchez-Cabeza and Ruiz-Fernández (2012). Other dating models with less restrictive assumptions are the Sediment Isotope Tomography (SIT) model (Carroll and Lerche, 2003) and the TERESA model (Abril, 2016).

It is not rare to find applications of the  $^{210}\text{Pb}$  method ignoring the complexities of sedimentary processes such as compaction, local mixing (physical mixing or bioturbation), erosion or episodic sedimentation that can significantly disturb the  $^{210}\text{Pb}$  profile and compromise the fundamental principles of the  $^{210}\text{Pb}$  dating models used. Different processes act to influence excess  $^{210}\text{Pb}$  ( $^{210}\text{Pb}_{\text{xs}}$  is the difference between total  $^{210}\text{Pb}$  and supported  $^{210}\text{Pb}$  in equilibrium with  $^{226}\text{Ra}$ ) vertical profile (Baskaran et al., 2014; Hancock et al., 2002; Delbono et al., 2016; Drexler and Nittrouer, 2008; Abril and Gharbi, 2012). Therefore, the

interpretation of  $^{210}\text{Pb}$  profiles is a complex process that requires proper choice of an appropriate  $^{210}\text{Pb}$  dating model. In many cases, both the identification of sedimentary processes and the limitations on the use of specific  $^{210}\text{Pb}$  dating models are not considered, nor properly discussed. In particular, the signals of post-depositional processes in  $^{210}\text{Pb}$  activity profiles, such as bioturbation or compaction during sampling, are often overlooked, thus overestimating sedimentation rates and producing questionable chronologies.

The issues discussed above have been released by other authors previously. For example, Hancock et al. (2002) highlighted that it is very common in scientific papers to assume that the  $^{210}\text{Pb}$  method is simple and it is no longer necessary to publish how the age-depth relationship (age model) was derived, and  $^{210}\text{Pb}$  dates are given without enough details (sometimes even without associated uncertainties). Therefore, many peer-reviewed papers on the reconstruction of contaminant concentrations and/or fluxes to sediment cores based on  $^{210}\text{Pb}$  chronologies lack the information required for proper evaluation by the expert reader. Sometimes, discussions are based on unavailable age-models that cannot be reproduced. For these reasons, suggestions for an editorial policy, regarding the use of  $^{210}\text{Pb}$  for sediment geochronology, were invoked by Smith (2001) who proposed standards for publication of  $^{210}\text{Pb}$  results, including an independent variable (such as  $^{137}\text{Cs}$  or other temporal marker as oil spills, metals, pollen profiles and sterols) to validate  $^{210}\text{Pb}$  profiles. The use of  $^{137}\text{Cs}$  activity profiles to validate  $^{210}\text{Pb}$  chronologies is based on the  $^{137}\text{Cs}$  distribution pattern along a sediment core, in which the maximum value is assumed to be related to 1963–1964, the period of maximum atmospheric fallout  $^{137}\text{Cs}$  (Ritchie and McHenry, 1990).

In order to contribute towards improving the process to obtain reliable  $^{210}\text{Pb}$  chronologies, the International Atomic Energy Agency (IAEA) supported a four-year Coordinated Research Project (CRP) “Study of Temporal Trends of Pollution in Selected Coastal Areas by the Application of Isotopic and Nuclear Tools” (CRP code: K41016). The aim of this project is to critically review the use of natural environmental archives for investigating the historical trends of contaminants in the marine environment and to show how the application of radioanalytical, isotopic and tracer techniques, in particular the  $^{210}\text{Pb}$  dating method, can contribute to producing reliable chronologies on the temporal behaviour of contaminants in coastal marine systems if properly applied. Participating countries in the project are Australia, Brazil, Italy, Jordan, Kenya, Kuwait, Malaysia, Mexico, Morocco, Russian Federation, Spain, Sri Lanka, Sweden and Vietnam.

A  $^{210}\text{Pb}$  dating modelling interlaboratory comparison exercise was carried out among the following laboratories: Australian Nuclear Science and Technology Organization (ANSTO)-Australia, Pontificia Universidade Católica do Rio de Janeiro-Brazil, Centro Interdisciplinar de Energia e Ambiente (CIENAM) Universidade Federal da Bahia-Brazil, the Italian National Agency for New Technologies Energy and Sustainable Economic Development (ENEA)-Italy, the University of Jordan and Marine Science Station (MSS)-Jordan, Kenya Marine and Fisheries Research Institute (KMFRI)-Kenya, Kuwait Institute for Scientific Research (KISR)-Kuwait, Malaysian Nuclear Agency-Malaysia, Instituto de Ciencias del Mar y Limnología Universidad Nacional Autónoma de México-Mexico, Centre National de l’Energie, des Sciences et des Techniques Nucléaires (CNESTEN)-Morocco, Universidad de Sevilla-Centro Nacional de Aceleradores-Spain, Linköping University-Sweden, Vietnam Atomic Energy Institute-Vietnam and Radiometrics Laboratory-Environment Laboratories IAEA-Monaco.

The main aim of this study was to evaluate the results of the interlaboratory comparison exercise to identify possible problems, limitations and constraints associated with the use of  $^{210}\text{Pb}$  dating models in order to provide guidelines and recommendations to improve the chronological reconstruction.

## 2. Methodology

Activity profiles of  $^{210}\text{Pb}$  and  $^{137}\text{Cs}$  in sediment cores were used by

each participating laboratory to produce  $^{210}\text{Pb}$  chronologies. The sediment cores were collected from two depositional settings in Australia: (1) a coastal shallow mangrove environment sampled in 2014 at a water depth < 5 m, with a core length of 30 cm and a sediment sub-sampling interval of 1 cm for the whole core; and (2) a tropical freshwater lake at an altitude of 850 m sampled in 2010 at ~30 m depth, core length of 45 cm and sampling resolution of 2 cm from the surface down to 24 cm, and 4 cm thereafter. The sediment samples after being sectioned, were freeze-dried and ground to powder by using porcelain mortars and pestles; except the aliquots to be used for grain size analysis.

Activities of  $^{210}\text{Pb}$  and  $^{137}\text{Cs}$  for the exercise were provided by ANSTO, which has ISO 9001 accreditation and is member of the IAEA Analytical Laboratories for the Measurement of Environmental Radioactivity (ALMERA) network. The analyses were carried out using both alpha-particle spectrometry (for  $^{210}\text{Pb}$  activities, determined through the radioactive descendant  $^{210}\text{Po}$ , assuming secular equilibrium between both radionuclides) and gamma-ray spectrometry (for  $^{210}\text{Pb}$ ,  $^{226}\text{Ra}$  and  $^{137}\text{Cs}$  activities). All laboratories received the following data for the sediment core sections: sample ID, cutting depths (cm), dry bulk density ( $\text{g cm}^{-3}$ ), counting date, activities and absolute uncertainties of total  $^{210}\text{Pb}$  ( $^{210}\text{Pb}_{\text{tot}}$ ,  $\text{Bq kg}^{-1}$ ), supported  $^{210}\text{Pb}$  (assumed at equilibrium with  $^{226}\text{Ra}$ ,  $\text{Bq kg}^{-1}$ ), and  $^{137}\text{Cs}$  ( $\text{Bq kg}^{-1}$ ), in addition to the sampling date and the water column depth of the sampling site.

For the coastal shallow mangrove sediment core, the analysed sections were 8 for  $^{210}\text{Pb}$  and 6 for  $^{137}\text{Cs}$ , close to the position of its maximum activity. Fig. 1 shows the activity profiles of  $^{210}\text{Pb}_{\text{tot}}$ ,  $^{226}\text{Ra}$ ,  $^{137}\text{Cs}$  and dry bulk density. The silt and clay percentages for each section were also provided (Supplementary material, Table 2). The  $^{210}\text{Pb}_{\text{tot}}$  profile (Fig. 1a) exhibits a subsurface maximum in the 5–6 cm section and an exponential trend below. Ra-226 (Fig. 1a) had relatively low activities, with a mean of  $3.1 \pm 0.9 \text{ Bq kg}^{-1}$ . The  $^{137}\text{Cs}$  profile (Fig. 1b) showed a sharp peak in section 16–17 cm. The dry bulk density depth profile (Fig. 1c) was almost constant down to 10 cm ( $0.18 \text{ g cm}^{-3}$ ) and then showed a gradual downwards increase, up to  $1.5 \text{ g cm}^{-3}$ .

For the lacustrine sediment core, twelve sub-samples were analysed for  $^{210}\text{Pb}$ , and seven for  $^{137}\text{Cs}$ . Fig. 2 shows the profiles of  $^{210}\text{Pb}_{\text{tot}}$ ,  $^{226}\text{Ra}$ ,  $^{137}\text{Cs}$  and dry bulk density. Activity profile of  $^{210}\text{Pb}_{\text{tot}}$  (Fig. 2a) shows a monotonic decrease from the core top to 18 cm, and below  $^{210}\text{Pb}_{\text{tot}}$  values show an almost constant trend until the core bottom, without reaching equilibrium with  $^{226}\text{Ra}$  activities (i.e.  $^{210}\text{Pb}_{\text{xs}}$  activity was not zero at the core bottom). Activity profile of  $^{226}\text{Ra}$  (Fig. 2a) was rather constant, with a mean value of  $217 \pm 39 \text{ Bq kg}^{-1}$ . Activity profile of  $^{137}\text{Cs}$  (Fig. 2b) shows a maximum value of  $8.4 \pm 0.8 \text{ Bq kg}^{-1}$  for the 15–16 cm section. Its activity decreased rapidly to values lower than the Minimum Detectable Activity (MDA) at section 22–23 cm. The dry bulk density depth profile (Fig. 2c) was almost constant ( $1.0 \pm 0.2 \text{ g cm}^{-3}$ ),

except for two similar values ( $1.44$  and  $1.41 \text{ g cm}^{-3}$ ) at 8–10 and 16–18 cm, respectively.

The participating laboratories submitted their dating results in a standard IAEA format, which included for each sediment section: sample ID, cutting depth (cm), mid-depth (cm), massic activity ( $\text{Bq kg}^{-1}$ ) and midpoint section age (years), both for  $^{210}\text{Pb}$  and  $^{137}\text{Cs}$  (uncertainties with coverage factor  $k = 1$ , i.e. one standard deviation). In addition, for each sediment core, participants prepared a separate document with: a) description of the model applied for dating, including chronology equations and the main dating assumptions; b) description of the procedure used for uncertainty calculations; c) average sediment accumulation rates, indicating time interval/depth interval of application; d) representation of the evolution of the sediment accumulation rate with depth/mass depth/age, if applicable; e) estimation of the  $^{210}\text{Pb}_{\text{xs}}$  inventory ( $\text{Bq m}^{-2}$ ) in the sediment column, or the  $^{210}\text{Pb}_{\text{xs}}$  flux; and (f) any additional information that the laboratory considered of interest.

### 3. Results

The age models for the two sediment cores are provided in the Supplementary Material section (Table 1). Regarding the other  $^{210}\text{Pb}$  dating derived data, the following results were provided: the average sedimentation rates were reported by 10 laboratories, the mass and/or sediment accumulation rate trends were reported by 7 laboratories, the value of  $^{210}\text{Pb}_{\text{xs}}$  inventory ( $\text{Bq m}^{-2}$ ) and/or  $^{210}\text{Pb}_{\text{xs}}$  flux were reported by 9 laboratories.

#### 3.1. Coastal sediment core

Participating laboratories carried out the  $^{210}\text{Pb}$  dating exercise using different approaches. Eight laboratories used the CFCS dating model, three laboratories used the CF model, two laboratories used modified versions of the CFCS model, while one lab used the CA model. Fig. 3a shows the reported age models while Fig. 3b shows the ages and uncertainties for two specific sections of the sediment core, one near the water-sediment interface (5–6 cm) and the other one near the core bottom (24–25 cm). Divergent results are evident in Fig. 3b.

#### 3.2. Freshwater lacustrine sediment core

For the freshwater lacustrine sediment core, seven laboratories used the CF model, five laboratories used the CFCS model, one laboratory used the CA model and another laboratory used a modified version of the CFCS model. Fig. 4a shows the reported age models while Fig. 4b shows the ages and associated uncertainties for two specific sections of the sediment core, one from the upper part of the core (8–10 cm) and the

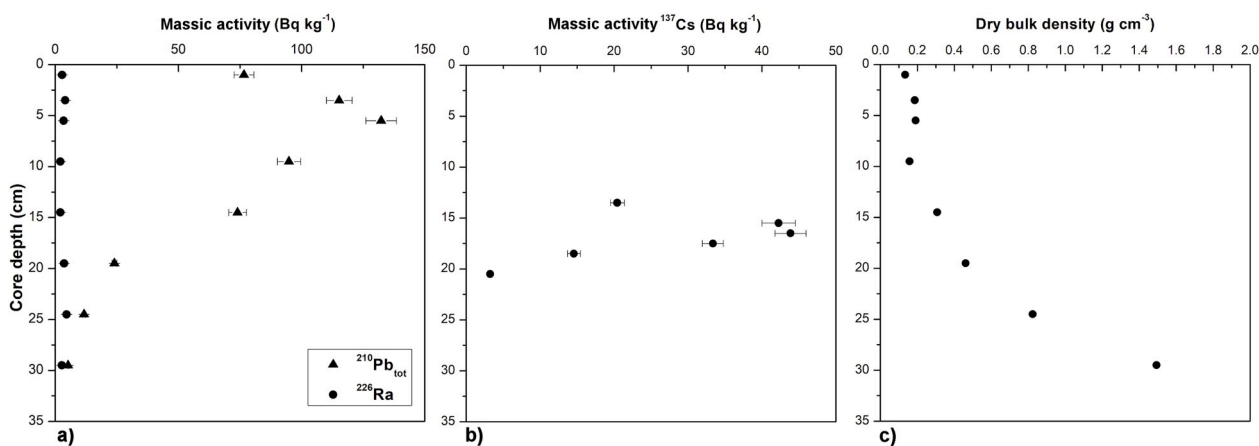


Fig. 1. Coastal sediment core: data provided for the  $^{210}\text{Pb}$  dating interlaboratory comparison exercise. Depth profiles of: a) total  $^{210}\text{Pb}$  and  $^{226}\text{Ra}$  activities; (b)  $^{137}\text{Cs}$  activities and (c) dry bulk density.

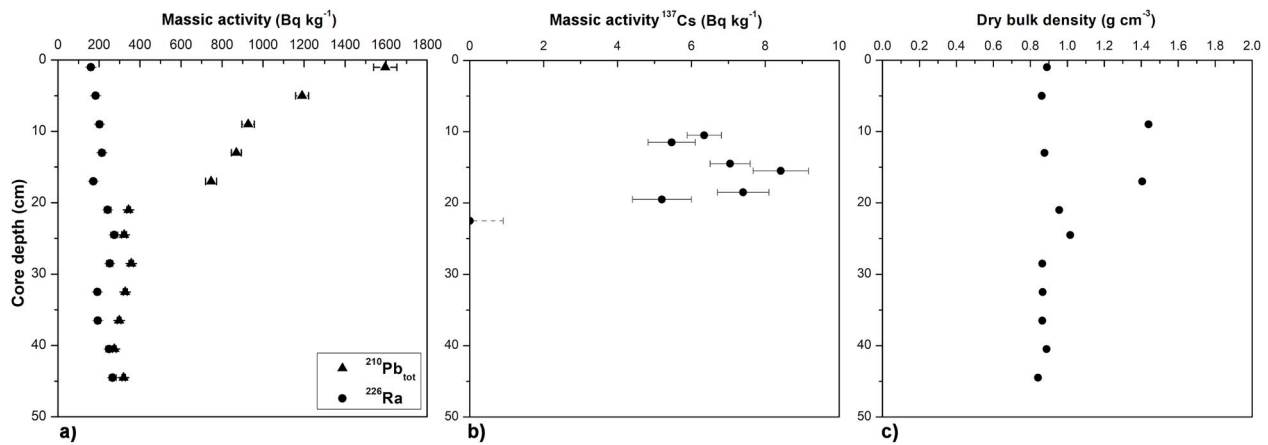


Fig. 2. Tropical freshwater lacustrine sediment core: data provided for the  $^{210}\text{Pb}$  dating interlaboratory comparison exercise. Depth profiles of: a) total  $^{210}\text{Pb}$  and  $^{226}\text{Ra}$  activities; b)  $^{137}\text{Cs}$  activities and c) dry bulk density. The dashed error bar of the deepest point of the  $^{137}\text{Cs}$  profile indicates the Minimum Detectable Activity (MDA) value.

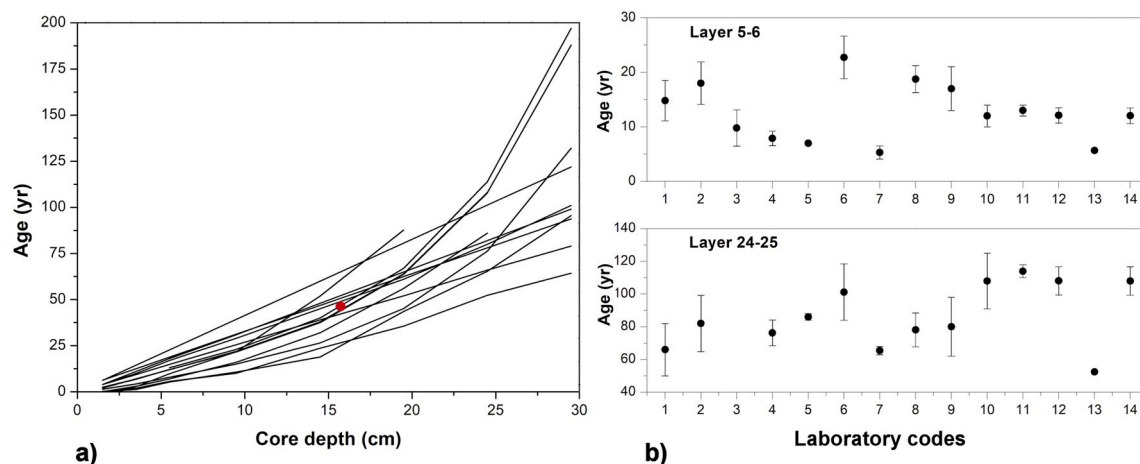


Fig. 3.  $^{210}\text{Pb}$  dating results for the coastal sediment core from the interlaboratory comparison exercise. (a) Reported age models; the red dot indicates the depth corresponding to  $^{137}\text{Cs}$  maximum activity value (1963). (b) Sediment ages at two specific core sections (5–6 cm above and 24–25 cm below). (For interpretation of the references to colour in this figure legend, the reader is referred to the Web version of this article.)

other one near the core bottom (36–37 cm). For both sections, the results provided by the participants are also quite divergent (see Fig. 4b).

For both data sets (the coastal and lake sediment cores), the treatment and the estimations of uncertainties associated to the given ages were applied differently among laboratories, thus reporting both very low and high values. It is evident that, despite the large quantity of publications on this topic, the age determination of sediments throughout the  $^{210}\text{Pb}$  method requires a standardized protocol. In this regard, a detailed discussion of the estimation of uncertainties is beyond the objectives of the present manuscript.

#### 4. Discussion

Since each laboratory was provided with the same numeric dataset, a completely standardized procedure for  $^{210}\text{Pb}$  dating should assure unique results (age model and sediment accumulation rates) for each core. Nevertheless, different decisions were made by different laboratories with regard to the choice of dating model, thus, yielding different results. A combination of the chosen model and its specific application has caused the observed dispersions (Figs. 3 and 4).

The most widely used  $^{210}\text{Pb}$  dating models are based on the common basic assumption that, when a layer is formed, the  $^{210}\text{Pb}_{\text{xs}}$  concentration is proportional to  $^{210}\text{Pb}_{\text{xs}}$  flux to the sediment surface and inversely

proportional to the mass accumulation rate, but also each model has its own specific assumptions and limitations that should be considered before use (as described in Sanchez-Cabeza and Ruiz-Fernández 2012).

The practical procedures that may affect dating results include: (i) the use of constant or weighted uncertainties in the  $^{210}\text{Pb}$  activity versus depth fitting procedure for the CFCS model, (ii) the handling of constant  $^{210}\text{Pb}$  activities at the core top (the so-called surface mixed layer), or increase downcore forming a sub-surface maximum (as observed in the coastal core, Fig. 1a), (iii) the overlooking of compaction effects on the linear depth scale, and (iv) the normalization of  $^{210}\text{Pb}$  activity values to compensate the effects of sediment grain size variations. In the case of the CF model, the interpolation protocol should be also considered to fill missing  $^{210}\text{Pb}$  activity values (not analysed sections) and the choice of the equilibrium depth (where  $^{210}\text{Pb}_{\text{xs}}$  activities are negligible), for an accurate estimation of the  $^{210}\text{Pb}_{\text{xs}}$  inventories.

Owing to the different choices of models and the different approaches to implement them,  $^{210}\text{Pb}$  chronologies should be validated (Smith, 2001). Depth profiles of  $^{137}\text{Cs}$  are expected to show a single well resolved peak (particularly in the Northern Hemisphere) corresponding to 1963, the year of maximum  $^{137}\text{Cs}$  fallout resulting from atmospheric testing of nuclear weapons (UNSCEAR, 2000), and when the signal is clear,  $^{137}\text{Cs}$  profile is commonly used. In the sampling area (Southern Hemisphere), peaks related to nuclear accidents at Chernobyl (1986) or

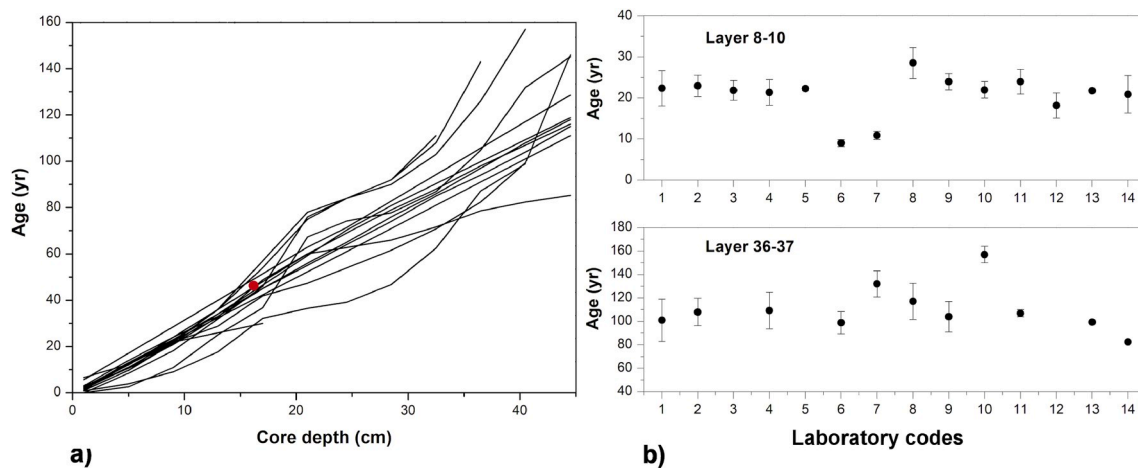


**Fig. 4.** a)  $^{210}\text{Pb}$  dating results for the fresh water lake sediment core from the interlaboratory comparison exercise. (a) Age patterns reported by all participating laboratories; the red dot indicates the depth corresponding to  $^{137}\text{Cs}$  maximum activity value (1963). (b) Age values at two specific core sections (8–10 cm above and 36–37 cm below) provided by the laboratories. (For interpretation of the references to colour in this figure legend, the reader is referred to the Web version of this article.)

Fukushima (2011) are not expected.  $^{137}\text{Cs}$  maxima could have been used as a chronostratigraphic marker to confirm the  $^{210}\text{Pb}$  derived age model, or to correct the model and assumptions during dating. However,  $^{137}\text{Cs}$  massic activity depth profiles might have also been altered by catchment-derived inputs, post-depositional remobilization, organic matter degradation or even in some cases,  $^{137}\text{Cs}$  activity might be below the detection limit (Ruiz-Fernández et al., 2012; Ruiz Fernández et al., 2019 and references therein). In the two analysed cases,  $^{137}\text{Cs}$  profile showed sharp peaks, likely implying negligible migration and diffusion.

#### 4.1. Coastal sediment core

Despite the availability of  $^{137}\text{Cs}$  data, only 8 out of 14 participating laboratories used  $^{137}\text{Cs}$  depth profiles to validate their age models. Commonly, the  $^{210}\text{Pb}$  derived age interval (considering dating uncertainties) of the core section in which the  $^{137}\text{Cs}$  maximum was identified, was contrasted against the date of maximum  $^{137}\text{Cs}$  fallout (i.e. 1963). If the  $^{210}\text{Pb}$  derived age diverges from 1963 to 1964, the  $^{210}\text{Pb}$  dating process should be revised. The dispersion of the mean age from all laboratories was about two-fold the dispersion of the mean age from dates corroborated with  $^{137}\text{Cs}$  (Fig. 5). When the  $^{137}\text{Cs}$  constraint was used, the dispersion of the age models was mostly reduced within the uppermost (20 cm) core sections. This exercise confirms and helps to better understand the effectiveness of the use of  $^{137}\text{Cs}$  profiles to corroborate the  $^{210}\text{Pb}$  age model. Fig. 5b could be considered as the “consensus value” of these laboratories, with excellent agreement back to ~60 years.

In order to better understand other causes of data dispersion, discussion below is restricted to the laboratories that validated the  $^{210}\text{Pb}$  age model with  $^{137}\text{Cs}$ . Fig. 6a shows the dating results of the 8 laboratories depending on the  $^{210}\text{Pb}$  dating model employed. From the 8 laboratories, only one used the CF model while seven laboratories used the CFCS model, from which four laboratories used the mass depth scale ( $\text{g cm}^{-2}$ ) and one of the remaining three laboratories used a correction for sediment compaction of the linear depth (Fig. 6a). The observed age dispersion was larger below ~20 cm depth, mainly caused by the use or non-use of mass depth to compensate for compaction effects in the CFCS model. The CF model results were not affected by the depth scale, as it was based on  $^{210}\text{Pb}_{\text{xs}}$  accumulated inventories (Sanchez-Cabeza and Ruiz-Fernández, 2012).

The divergence of the CFCS dating results is related to dry bulk density changes along the core (Fig. 1c). In this coastal core, the sediment is characterized by changes of the dry bulk density of about one

order of magnitude, hence compaction effects should not be neglected (Fig. 6b). Since the CFCS model is based on the linear regression analysis between  $\ln^{210}\text{Pb}_{\text{xs}}$  and sediment depth, the choice between linear or mass depth scales provides quite different ages. In fact, age models in Fig. 6a using the mass depth followed the mass depth *versus* linear depth trend in Fig. 6b. When applying the CFCS model to establish a  $^{210}\text{Pb}$  chronology, the use of mass depth (instead of linear depth) is strongly recommended (Binford, 1990; Sanchez-Cabeza and Ruiz-Fernández, 2012), as clearly shown in this exercise.

The use of the core top  $^{210}\text{Pb}$  data also produced some age dispersion (~1.5 times the uncertainty, Fig. 5b). The  $^{210}\text{Pb}$  profile showed a maximum in the third section (5.5 cm depth), and this led to various approaches by the laboratories using the CFCS model, but not for the CF model which attributes  $^{210}\text{Pb}$  activity changes to radioactive decay and changes of sediment accumulation. One process that may explain the observed near-surface  $^{210}\text{Pb}$  activity distribution is the presence of sediment components (such as a carbonate or organic fraction, not available in this exercise) that might dilute  $^{210}\text{Pb}$  and  $^{226}\text{Ra}$  activities; or higher sediment loads which would dilute the  $^{210}\text{Pb}_{\text{xs}}$  concentrations. Since there was no significant variation of  $^{226}\text{Ra}$  activities along the core (Fig. 1a), sediment composition may be considered homogeneous and hence there was no need for normalization of  $^{210}\text{Pb}$  activities before applying the CFCS model. When using the CFCS model, three laboratories performed the best fitting calculation by rejecting the first two sediment sections, one laboratory discarded the core top section and three laboratories did not reject any section. The potential presence of post-depositional mixing processes, such as bioturbation, may also explain the irregular trend near the surface (Cochran and Masqué, 2003). One laboratory used the non-ideal deposition model (Abril and Gharbi, 2012) for the two first sections, and the CFCS model below. Finally, one laboratory used a linear regression weighted with uncertainties (Taylor, 1997).

In brief, the main sources of dispersion in modeled ages for the coastal sediment core were: 1) the lack of use of  $^{137}\text{Cs}$  activities to validate the  $^{210}\text{Pb}$ -derived age model; 2) the lack or erroneous correction of sediment compaction effects on the core depth; and 3) application of different approaches to interpret the irregular trend of  $^{210}\text{Pb}_{\text{xs}}$  in surface sections, although this did not produce a significant dispersion, most likely due to its small thickness (4 cm).

In general, the main dispersion sources are strongly conditioned by the  $^{210}\text{Pb}_{\text{xs}}$  activity profile, such as discontinuities or a profile different from an exponential decrease, so that a careful application of the  $^{210}\text{Pb}$  dating model is required by radiochronologists.

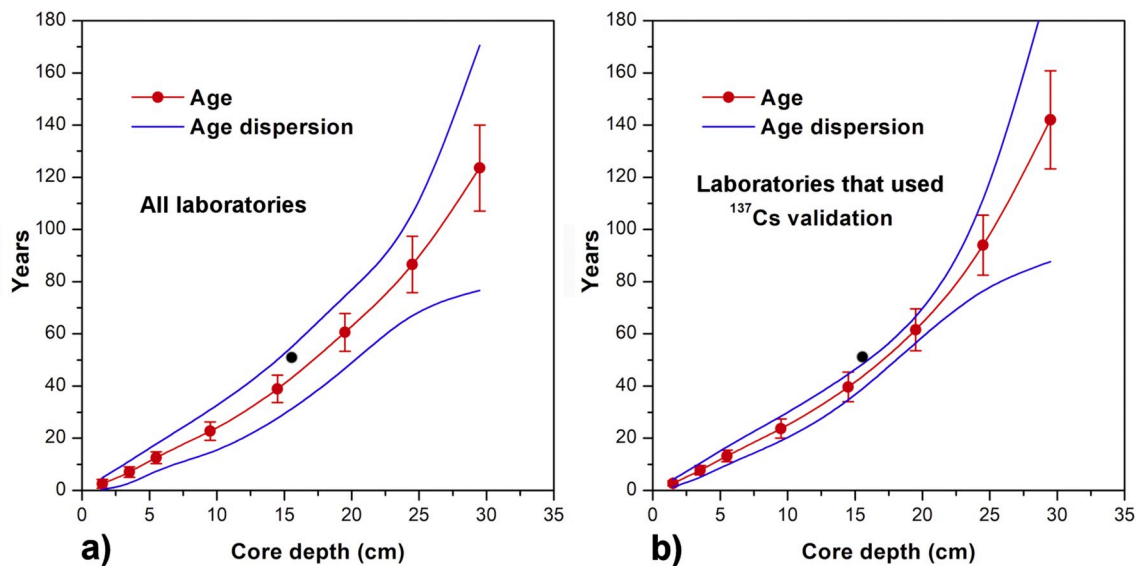


**Fig. 5.** Coastal sediment core used for interlaboratory comparison exercise. Mean age and uncertainty for each sediment section (red line and error bars, respectively), and age dispersion (age  $\pm$  age standard deviation, blue lines) for (a) all laboratories, and (b) laboratories using  $^{137}\text{Cs}$  data to validate the  $^{210}\text{Pb}$ -derived age model. The black dot indicates the depth corresponding to  $^{137}\text{Cs}$  maximum activity value (1963). (For interpretation of the references to colour in this figure legend, the reader is referred to the Web version of this article.)

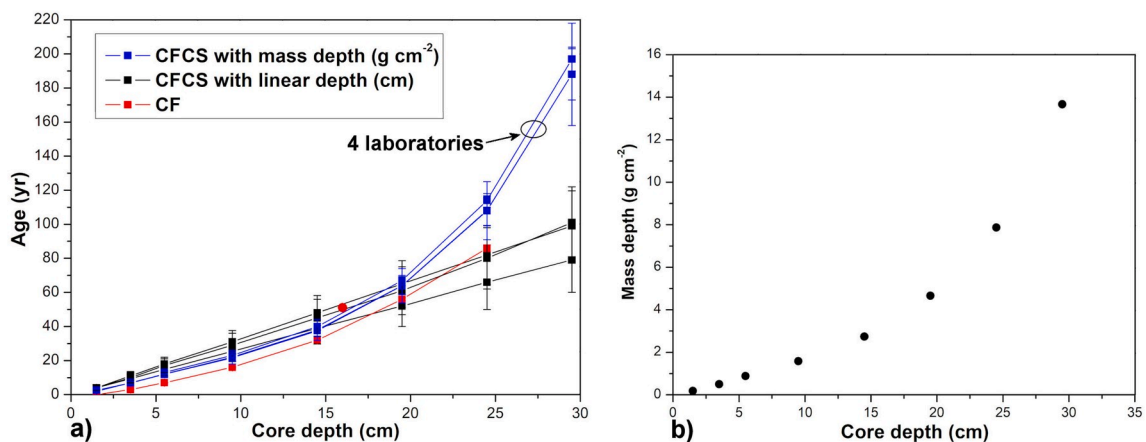


**Fig. 6.** Coastal sediment core used for interlaboratory comparison exercise. (a) Age models of the 8 laboratories that used the  $^{137}\text{Cs}$  profile for  $^{210}\text{Pb}$  dating validation. Blue lines indicate the four laboratories that used mass depth ( $\text{g cm}^{-2}$ ) to apply the CFCS model (the age modeled curves are two by two coincident); black lines indicate the three laboratories that used linear depth (cm) to apply the CFCS model, and the red line indicates the only laboratory that used the CF dating model; the red dot indicates the depth corresponding to  $^{137}\text{Cs}$  maximum activity value (1963). (b) Relationship between mass depth and linear depth in the coastal sediment core. (For interpretation of the references to colour in this figure legend, the reader is referred to the Web version of this article.)

#### 4.2. Freshwater lacustrine sediment core

The lacustrine sediment core also showed a large dispersion of  $^{210}\text{Pb}$  ages (Fig. 4). Similar to the coastal sediment core, Fig. 7a shows mean age and uncertainty values for each sediment layer for all laboratories, and Fig. 7b illustrates the mean age and uncertainty values for each sediment section for the laboratories that used the  $^{137}\text{Cs}$  profile to validate the  $^{210}\text{Pb}$  dating method (8 out of 14 laboratories).

The average age values for the two groups of laboratories were similar (Fig. 7a and b, red lines), while significant differences (11 years in section 44–45 cm) were only observed in the deepest sediment sections. The age dispersion among all laboratories is wider than the uncertainties for each age (Fig. 7a), while the contrary was observed for laboratories that validated their dating with  $^{137}\text{Cs}$  (Fig. 7b): the dispersion of dating results was less than or equal to the mean age uncertainty down to 18 cm; then it remained close to the experimental uncertainty down to 33 cm, and only below this depth the dispersion

became larger. It was concluded that the use of  $^{137}\text{Cs}$  to validate  $^{210}\text{Pb}$  dating considerably reduced the dispersion of the dating results. Fig. 7b could be considered as the “consensus” value of the laboratories using  $^{137}\text{Cs}$  validation, with excellent agreement back to  $\sim 50$  yr.

When considering only the laboratories that applied  $^{137}\text{Cs}$  validation, the dispersion curve diverged significantly from the mean error bars only at the core bottom (Fig. 7b). Four laboratories used the CFCS model, and the other four used the CF model (Fig. 8a). The relationship between depth and mass depth showed no slope change (Fig. 8b) indicating that the compaction effect was small, resulting in a good agreement among laboratories that used the CFCS model with (one laboratory) or without (three laboratories) compaction correction.

The age model dispersion for the deeper sections was largely caused by the chosen dating model (Fig. 8a). The shape of the  $^{210}\text{Pb}_{\text{xs}}$  profile (Fig. 2a) showed two segments separated by an abrupt decrease at 18–20 cm depth. The upper core segment (0–18 cm) had a continuous but decreasing trend, while the deeper segment (20–45 cm) exhibited a

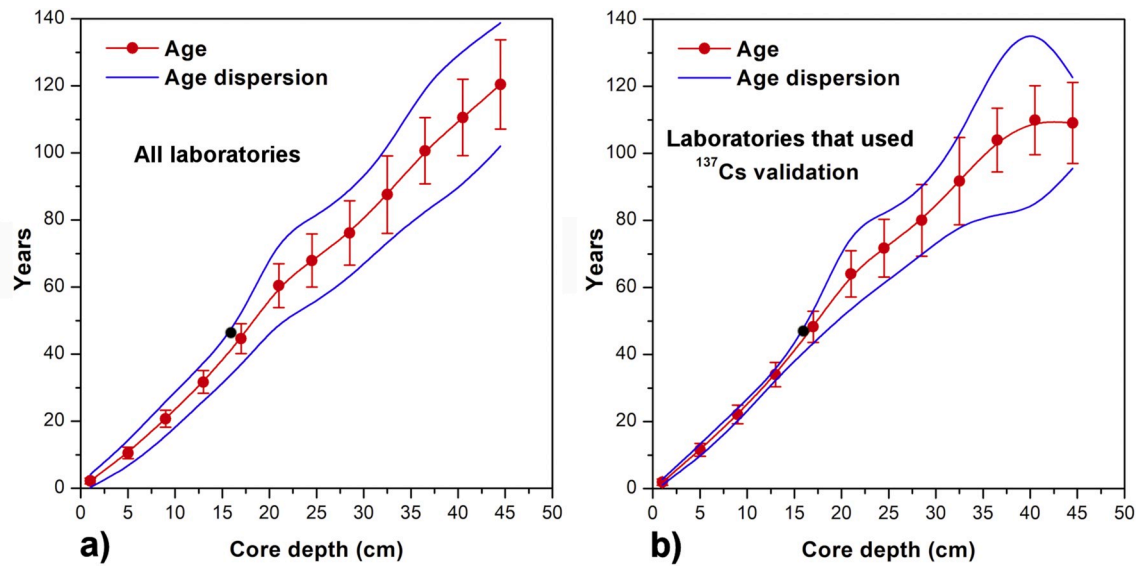


**Fig. 7.** Lacustrine sediment core used for interlaboratory comparison exercise. Mean age and uncertainty for each sediment section (red line and error bars, respectively) and age dispersion (mean age  $\pm$  standard deviation, blue lines) for (a) all laboratories and (b) laboratories that used  $^{137}\text{Cs}$  data to validate the  $^{210}\text{Pb}$ -derived age model. The black dot indicates the depth corresponding to  $^{137}\text{Cs}$  maximum activity value (1963). (For interpretation of the references to colour in this figure legend, the reader is referred to the Web version of this article.)

rather constant  $^{210}\text{Pb}_{\text{ex}}$  activity, close to zero. The  $^{137}\text{Cs}$  peak was observed above the discontinuity, limiting the validation of the CF and CFCS models only to the upper segment (about 60 years).

CF age model showed increasing dispersion with depth. The CF chronology equation is based on the knowledge of inventories below certain depths, so commonly interpolations were needed. The interpolation method chosen by each laboratory was therefore the main source of dispersion. Furthermore, the estimate of the depth where equilibrium is reached, is an additional difficulty since activities are commonly low and uncertainties high. This is clearly reflected in this exercise, as the chosen equilibrium sections are different among the laboratories (Fig. 8a). However, the age models converge above the  $^{210}\text{Pb}_{\text{xs}}$  profile discontinuity, since differences in  $^{210}\text{Pb}_{\text{xs}}$  inventories become negligible above it (Fig. 8a). The large uncertainties in the older sediments is a well-known and intrinsic problem of the CF model, since uncertainties increase exponentially with age (see Binford, 1990 for further discussion). Thus, it is advisable to keep the dating interval within time periods of one hundred years or so (Goldberg, 1963), since  $^{210}\text{Pb}_{\text{xs}}$  variations are

difficult to detect in sediments older than 110 years ( $\sim$ five half-lives of  $^{210}\text{Pb}$ ) and to improve uncertainty calculations, for example, by using Bayesian methods (Sanchez-Cabeza et al., 2014; Aquino-López et al., 2018). This discussion is also applicable to the CFCS model in which ages older than about 100 years should not be reported but considered as extrapolations.

Three CF model-derived age models also showed convergence, although with high uncertainties, at about 100 years. In the fourth case, the laboratory assumed that the inventory was not complete, and calculated the missing inventory, so ages extended to the core bottom and were younger than in the other cases (Fig. 8a). The used missing inventory was larger than the one corresponding to the deepest five sections.

This exercise helped to emphasize the advantages and disadvantages of CFCS and CF models. The CFCS model requires a stricter set of main assumptions, so its applicability is more limited. The CF model is applicable in a wider set of environments, but its chronologies are highly dependent on the choice of the  $^{210}\text{Pb}_{\text{xs}}$  equilibrium depth, and the age

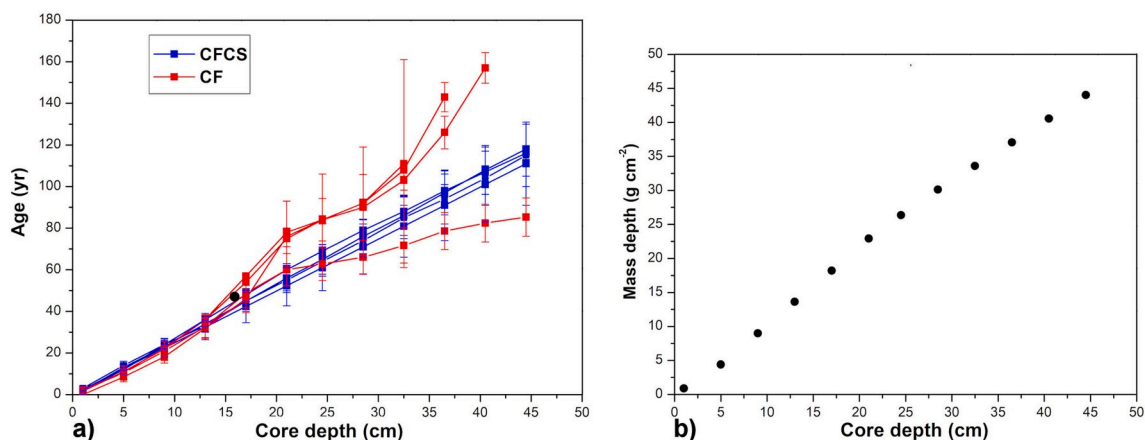


**Fig. 8.** Lacustrine sediment core used for interlaboratory comparison exercise. (a) Age models validated with  $^{137}\text{Cs}$  (eight laboratories). Blue lines refer to four laboratories that used the CFCS model; red lines refer to four laboratories that used the CF model; the black dot indicates the depth corresponding to  $^{137}\text{Cs}$  maximum activity value (1963). (b) Relationship between mass depth and linear depth along the core. (For interpretation of the references to colour in this figure legend, the reader is referred to the Web version of this article.)

uncertainties are specially large for the oldest sections of the core (where  $^{210}\text{Pb}_{\text{xs}}$  values approach to zero). To solve this, a validation older than the  $^{137}\text{Cs}$  maximum should be desirable (e.g. tephra, sedimentary events caused by strong meteorological events, onset of specific contaminants), even though it is not always easy to apply. A criterion to use the CF model is that the  $^{210}\text{Pb}_{\text{xs}}$  inventory should correspond to the standing crop of the direct atmospheric flux (Appleby and Oldfield, 1983; 1992) which is useful to evaluate if the  $^{210}\text{Pb}$  inventory or the  $^{210}\text{Pb}$  flux determined during the dating process is compatible with the values reported for the geographical region of interest (Turekian et al., 1977; Preiss et al., 1996; Liu et al., 2001; Ruiz-Fernández and Hillaire-Marcel, 2009; Carnero-Bravo et al., 2014). Grain size analyses were also provided in order to understand the  $^{210}\text{Pb}_{\text{xs}}$  profile variability owing to the changes in the grain size distribution. Studies elsewhere have demonstrated the usefulness of normalizing  $^{210}\text{Pb}$  activities to the clay contents in each sample before using the CFCS model (DeGeest et al., 2008; Palinkas and Nittrouer, 2007). The grain size of the lacustrine sediment core showed a weak decreasing trend of clay content with depth (28–24%; Supplementary material, Table 2), but there was no meaningful discontinuity. Consequently, normalization to the clay content did not affect the activity profile. The  $^{226}\text{Ra}$  profile (Fig. 2a) showed high concentrations and high variability, ranging between 150 and 280 Bq  $\text{kg}^{-1}$ , and a general increasing trend with depth. Such variations may indicate changes in sediment sources, which might be helpful to validate the chronologies.

In summary, the main sources of dispersion in model ages in the lacustrine core were: 1) the use (or not) of  $^{137}\text{Cs}$  profile to validate  $^{210}\text{Pb}$  age models; 2) the choice of the  $^{210}\text{Pb}$  dating model; and when applying the CF model: 3) the choice of the equilibrium depth; and 4) the estimation of  $^{210}\text{Pb}_{\text{ex}}$  missing inventory.

## 5. Conclusions and recommendations

This  $^{210}\text{Pb}$  dating interlaboratory comparison modelling exercise highlighted some crucial aspects to be considered when attempting to obtain  $^{210}\text{Pb}$ -derived chronologies. Even though  $^{210}\text{Pb}$  sediment dating method is an excellent tool (and often the only available option), its appropriate application is critical for a large number of many environmental studies in order to establish recent (100–150 yr) sediment chronologies. However, dating models should not be used as routine tools, because each core may need a different approach, with enough confidence and verifiable evidence supporting the proposed chronologies. The good planning and execution of a study, including sophisticated analyses, could be futile if based on a poorly constrained or erroneous chronology. The correct understanding of each dating model, its assumptions and limitations in each environment is essential to provide reliable chronologies or declare a core as non-datable. This evaluation must start from a critical examination of the  $^{210}\text{Pb}_{\text{xs}}$  depth profile that should have, in an ideal case, a decreasing exponential trend. Irregular profiles and/or discontinuities must be evaluated, together with other indicators (such as the elemental composition, grain size), to understand if the depositional environment at the sampling site could meet the conceptual assumptions of the dating model, and if the profile responds to changing sedimentary conditions.

Through the analysis of the results from this interlaboratory comparison modelling exercise, some conclusions and remarks are highlighted herein. It is expected that they might contribute to the development of best practices to provide reliable environmental reconstructions:

- It is essential to compare the  $^{210}\text{Pb}$  chronology with some independent temporal markers to validate the age model. In this exercise, laboratories which did not validate their age model with  $^{137}\text{Cs}$  increased the age model dispersion by at least 30%; in the absence of a  $^{137}\text{Cs}$  peak, temporal profiles of other markers like oil spills, metals,

pollen, sterols or extreme events could effectively be used to validate  $^{210}\text{Pb}$  chronologies.

- It is strongly advisable to use more than one independent temporal marker for different core sections: in this way for  $^{210}\text{Pb}_{\text{xs}}$  depth profiles with irregular trends and/or discontinuities, it is possible to check whether the mass accumulation rate is constant in different segments of the sediment core, verifying the CFCS model. For the CFCS model, sediment compaction should be taken into account by using the mass depth ( $\text{g cm}^{-2}$ ) or a depth (cm) corrected for sediment compaction;
- In the case of irregular  $^{210}\text{Pb}_{\text{xs}}$  profiles (with abrupt changes or showing irregular departures from the typical exponential decay trend), it can be a good practice to normalize  $^{210}\text{Pb}_{\text{xs}}$  activities to the content of clay (or a geochemical proxy for textural variation such as aluminium) or organic matter, to reduce the influence of preferential adsorption by fine particles and organic matter;
- The choice of the interpolation method for missing data in the CF model, and the choice of the best fitting procedure for the CFCS model, can produce significantly different ages, although it is recognized that there is no standard procedure to solve this issue;
- If the assumptions of the CFCS and CF models are satisfied, the age model should be similar. If the equilibrium depth is clearly observable, the CF model should be used, since it requires only one environmental constraint (constant  $^{210}\text{Pb}_{\text{xs}}$  flux);
- The importance of the chronology uncertainties is usually underestimated, and a standard common protocol is needed for their proper determination.

In the framework of the IAEA Project “Study of temporal trends of pollution in selected coastal areas by the application of isotopic and nuclear tools” (CRP K41016), other interlaboratory comparison exercises on  $^{210}\text{Pb}$  dating are in progress in order to contribute to disseminate best practices for this widespread and important dating method of recent sediments.

## Acknowledgements

The IAEA is grateful to the Government of the Principality of Monaco for the support provided to its Environment Laboratories.

This work has been supported by the IAEA Coordinated Research project “Study of Global Temporal Trends of Pollution in Selected Coastal Areas by the Application of Isotopic and Nuclear Tools” (CRP K41016).

The paper is a collective effort of participants in IAEA’s CRP K41016 and their respective teams.

## Appendix A. Supplementary data

Supplementary data to this article can be found online at <https://doi.org/10.1016/j.quageo.2020.101093>.

## References

- Abril, J.M., Gharbi, F., 2012. Radiometric dating of recent sediments: beyond the boundary conditions. *J. Paleolimnol.* 48, 449–460.
- Abril, J.M., 2016. A  $^{210}\text{Pb}$ -based chronological model for recent sediments with random entries of mass and activities: model development. *J. Environ. Radioact.* 151, 64–74.
- Alonso-Hernandez, C.M., Tolosa, I., Mesa-Albernas, M., Diaz-Asencio, M., Corcho-Alvarado, J.A., Sanchez-Cabeza, J.A., 2015. Historical trends of organochlorine pesticides in a sediment core from the Gulf of Batabanó, Cuba. *Chemosphere* 137, 95–100.
- Appleby, P.G., Oldfield, F., 1978. The calculation of lead-210 dates assuming a constant rate of supply of unsupported  $^{210}\text{Pb}$  to the sediment. *Catena* 5, 1–8.
- Appleby, P.G., Oldfield, F., Thompson, R., Huttunen, P., Tolonen, K., 1979.  $^{210}\text{Pb}$  dating of annually laminated lake sediment from Finland. *Nature* 280, 53–55.
- Appleby, P.G., Oldfield, F., 1983. The assessment of  $^{210}\text{Pb}$  data from sites with varying sediment accumulation rates. *Hydrobiologia* 103, 29–35.
- Appleby, P.G., Oldfield, F., 1992. Application of lead-210 to sedimentation studies. In: Ivanovich, M., Harman, R.S. (Eds.), *Uranium-Series Disequilibrium: Application to Earth, Marine, and Environmental Sciences*. Clarendon Press, Oxford.



- Aquino-López, M.A., Blaauw, M., Christen, J.A., Sanderson, N.K., 2018. Bayesian analysis of  $^{210}\text{Pb}$  dating. *J. Agric. Biol. Environ. Stat.* 23 (3), 317–333.
- Arias-Ortiz, A., Masqué, P., García-Orellana, J., Serrano, O., Mazarrasa, I., Marbá, N., et al., 2018. Reviews and syntheses:  $^{210}\text{Pb}$ -derived sediment and carbon accumulation rates in vegetated coastal ecosystems - setting the record straight. *Biogeosciences* 15 (22), 6791–6818.
- Baskaran, M., Nix, J., Kuyper, C., Karunakara, N., 2014. Problems with the dating of sediment core using excess  $^{210}\text{Pb}$  in a freshwater system impacted by large scale watershed changes. *J. Environ. Radioact.* 138, 355–363.
- Binford, M.W., 1990. Calculation and uncertainty analysis of  $^{210}\text{Pb}$  dates for PIRLA project lake sediment cores. *J. Paleolimnol.* 3, 253–267.
- Carnero-Bravo, V., Merino-Ibarra, M., Ruiz-Fernández, A.C., Sanchez-Cabeza, J.A., Ghaleb, B., 2014. Sedimentary record of water column trophic conditions and sediment carbon fluxes in a tropical water reservoir (Valle de Bravo, Mexico). *Environ. Sci. Pollut. Control Ser.* 22 (6), 4680–4694.
- Carroll, J., Lerche, I., 2003. *Sedimentary Processes: Quantification Using Radionuclides*. Elsevier, Oxford.
- Cochran, J.K., Masqué, P., 2003. Short-lived U/Th series radionuclides in the ocean: tracers for scavenging rates, export fluxes and particle dynamics. *Rev. Mineral. Geochem.* 52 (1), 461–492.
- DeGeest, A.L., Mullenbach, B.L., Puig, P., Nittrouer, C.A., Drexler, T.M., Durrieu de Madron, X., Orange, D.L., 2008. Sediment accumulation in the western Gulf of Lions, France: the role of Cap de Creus Canyon in linking shelf and slope sediment dispersal systems. *Continent. Shelf Res.* 28, 2031–2047.
- Delbono, I., Barsanti, M., Schirone, A., Conte, F., Delfanti, R., 2016.  $^{210}\text{Pb}$  mass accumulation rates in the depositional area of the Magra River (Mediterranean Sea, Italy). *Continent. Shelf Res.* 124, 35–48.
- Drexler, T.M., Nittrouer, C.A., 2008. Stratigraphic signatures due to flood deposition near the rhone river: gulf of lions, northwest mediterranean sea. *Continent. Shelf Res.* 28, 1877–1894.
- GESAMP, 1987. Land/sea boundary flux of contaminants: contributions from rivers. *Rep. Stud.* 32, 172.
- GESAMP, 1994. Anthropogenic influences on sediment discharge to the coastal zone and environmental consequences. *Rep. Stud.* 52, 69.
- Goldberg, E.D., IAEA, 1963. *Geochronology with  $^{210}\text{Pb}$* . In: *Symp. Radioact. Dating. Int. Assoc. Hydrol. Sci. Publ.*, Vienna, Austria, pp. 122–130.
- Hancock, G., Edgington, D.N., Robbins, J.A., Smith, J.N., Brunskill, G., Pfitzner, J., 2002. Workshop on Radiological Techniques in Sedimentation Studies: Methods and Applications. Proceedings of the South Pacific Environmental Radioactivity Association (SPERA) 2000. IRD Edition, Paris, pp. 234–251.
- Koide, M., Soutar, A., Goldberg, E.D., 1972. Marine geochronology with  $^{210}\text{Pb}$ . *Earth Planet Sci. Lett.* 14, 442–446.
- Krishnaswamy, S., Lal, D., Martin, J.M., Meybeck, M., 1971. Geochronology of lake sediments. *Earth Planet Sci. Lett.* 11, 407–414.
- Liu, H., Jacob, D.J., Bey, I., Yantosca, R.M., 2001. Constraints from  $^{210}\text{Pb}$  and  $^7\text{Be}$  on wet deposition and transport in a global three-dimensional chemical tracer model driven by assimilated meteorological fields. *J. Geophys. Res.* 106, D11, 12,109–12,128.
- Martín, J., Sanchez-Cabeza, J.A., Eriksson, M., Levy, I., Miquel, J.C., 2009. Recent accumulation of trace metals in sediments at the DYFAMED site (Northwestern Mediterranean Sea). *Mar. Pollut. Bull.* 59 (4–7), 146–153.
- Miralles, J., Radakovitch, O., Cochran, J.K., Véron, A., Masqué, P., 2004. Multitracer study of anthropogenic contamination records in the Camargue, Southern France. *Sci. Total Environ.* 320, 63–72.
- Páez-Osuna, F., Álvarez-Borrego, S., Ruiz-Fernández, A.C., García-Hernández, J., Jara-Marini, M., Bergés-Tiznado, M.E., Piñón-Gimate, A., Alonso-Rodríguez, R., Soto-Jiménez, M.F., Frías-Espericueta, M.G., Ruelas-Inzunza, J.R., Green-Ruiz, C., Osuna-Martínez, C.C., Sanchez-Cabeza, J.A., 2017. Environmental status of the Gulf of California: a pollution review. *Earth Sci. Rev.* 166, 181–205.
- Palinkas, C.M., Nittrouer, C.A., 2007. Modern sediment accumulation on the Po shelf, Adriatic Sea. *Continent. Shelf Res.* 27, 489–505.
- Preiss, N., Mélières, M.A., Pourchet, M., 1996. A compilation of data on lead 210 concentration in surface air and fluxes at the air-surface and water-sediment interfaces. *J. Geophys. Res.* 101, D22, 28,847–28,862.
- Ritchie, J.C., McHenry, J.R., 1990. Application of radioactive fallout cesium-137 for measuring soil erosion and sediment accumulation rates and patterns: a review. *J. Environ. Qual.* 19, 215–223.
- Robbins, J.A., Edgington, D.N., 1975. Determination of recent sedimentation rates in Lake Michigan using Pb-210 and Cs-137. *Geochem. Cosmochim. Acta* 39, 285–304.
- Ruiz Fernández, A.C., Rangel-García, M., Perez Bernal, L.H., Lopez-Mendoza, P.G., Gracia, A., Schwing, P., Hollander, D., Páez-Osuna, F., Cardoso-Mohedano, J.G., Cuellar-Martínez, T., Sanchez-Cabeza, J.A., 2019. Mercury in sediment cores from the southern Gulf of Mexico: preindustrial levels and temporal enrichment trends. *Mar. Pollut. Bull.* 149 <https://doi.org/10.1016/j.marpolbul.2019.110498>.
- Ruiz-Fernández, A.C., Hillaire-Marcel, C., 2009.  $^{210}\text{Pb}$ -derived ages for the reconstruction of terrestrial contaminant history into the Mexican Pacific coast: potential and limitations. *Mar. Pollut. Bull.* 59, 134–145.
- Ruiz-Fernández, A.C., Sanchez-Cabeza, J.A., Alonso-Hernández, C., Martínez-Herrera, V., Pérez-Bernal, L.H., Preda, M., Hillaire-Marcel, C., Gastaud, J., Quejido-Cabezas, A.J., 2012. Effects of land use change and sediment mobilization on coastal contamination (Coatzacoalcos River, Mexico). *Continent. Shelf Res.* 37, 57–65.
- Sanchez-Cabeza, J.A., Druffel, E.R., 2009. Environmental records of anthropogenic impacts on coastal ecosystems: an introduction. *Mar. Pollut. Bull.* 59, 87–90, 2009.
- Sanchez-Cabeza, J.A., Ruiz-Fernández, A.C., 2012.  $^{210}\text{Pb}$  sediment radiochronology: an integrated formulation and classification of dating models. *Geochem. Cosmochim. Acta* 82, 183–200.
- Sanchez-Cabeza, J.A., Ruiz-Fernández, A.C., Ontiveros-Cuadras, J.F., Pérez-Bernal, L.H., Olid, C., 2014. Monte Carlo uncertainty calculation of  $^{210}\text{Pb}$  chronologies and accumulation rates of sediments and peat bogs. *Quat. Geochronol.* 23, 80–93. <https://doi.org/10.1016/j.quageo.2014.06.002>.
- Smith, J.N., 2001. Why should we believe  $^{210}\text{Pb}$  sediment geochronologies? *J. Environ. Radioact.* 55, 121–123.
- Taylor, J.R., 1997. *Introduction to Error Analysis: the Study of Uncertainties in Physical Measurements, A Series of Books in Physics*. University Science Books.
- Turekian, K.K., Nozaki, Y., Benninger, L.K., 1977. Geochemistry of atmospheric radon and radon products. *Annu. Rev. Earth Planet Sci.* 5, 227–255.
- Turner, S., Horton, A.A., Rose, N.L., Hall, C., 2019. A temporal sediment record of microplastics in an urban lake, London, UK. *J. Paleolimnol.* 61, 449–462.
- UNSCEAR, 2000. Annex C: exposures to the public from man-made sources of radiation. Report of the United Nations Scientific Committee on the Effects of Atomic Radiation.